Nanoscale Research Letters
a SpringerOpen Journal

NANO EXPRESS   **Open Access**

Low-temperature growth of highly crystalline β-Ga₂O₃ nanowires by solid-source chemical vapor deposition

Ning Han[1,3], Fengyun Wang[2], Zaixing Yang[1,3], SenPo Yip[1,3], Guofa Dong[1], Hao Lin[1,3], Ming Fang[1], TakFu Hung[1] and Johnny C Ho[1,3*]

Abstract

Growing Ga₂O₃ dielectric materials at a moderately low temperature is important for the further development of high-mobility III-V semiconductor-based nanoelectronics. Here, β-Ga₂O₃ nanowires are successfully synthesized at a relatively low temperature of 610°C by solid-source chemical vapor deposition employing GaAs powders as the source material, which is in a distinct contrast to the typical synthesis temperature of above 1,000°C as reported by other methods. In this work, the prepared β-Ga₂O₃ nanowires are mainly composed of Ga and O elements with an atomic ratio of approximately 2:3. Importantly, they are highly crystalline in the monoclinic structure with varied growth orientations in low-index planes. The bandgap of the β-Ga₂O₃ nanowires is determined to be 251 nm (approximately 4.94 eV), in good accordance with the literature. Also, electrical characterization reveals that the individual nanowire has a resistivity of up to 8.5×10^7 Ω cm, when fabricated in the configuration of parallel arrays, further indicating the promise of growing these highly insulating Ga₂O₃ materials in this III-V nanowire-compatible growth condition.

Keywords: β-Ga₂O₃ nanowires; Chemical vapor deposition; Solid-source; Highly crystalline; Large resistance; Dielectric

PACS: 77.55.D; 61.46.Km; 78.40.Fy

Background

In the past decade, gallium oxide (Ga₂O₃), as a large-bandgap (approximately 4.9 eV) semiconductor, has attracted extensive attention in the area of insulating oxides for the metal-oxide-semiconductor (MOS) technology as well as the active materials for the solar-blind deep ultraviolet detectors [1-6]. In particular, when high-mobility III-V compound semiconductor nanomaterials, such as GaAs, InAs, GaSb, and InSb nanowires (NWs), have been successfully illustrated with their great technological potentials in next-generation electronics [7-9], Ga₂O₃-based gate dielectrics are of significant importance to be achieved and to outperform the

conventional silicon technology, due to their excellent stability and relatively high dielectric constant (approximately 14.2) as compared to that of SiO₂ (approximately 3.9) or even the typically used high-κ Al₂O₃ (approximately 8) [1,10].

Till now, there are several effective integrations of Ga₂O₃-based gate dielectrics demonstrated in thin-film III-V field-effect transistors (FETs). For instance, Ga₂O₃ and Ga₂O₃/Gd₂O₃ composite materials have been shown to be excellent gate dielectrics for GaAs, In$_x$Ga$_{1-x}$As, and GaN thin-film transistors with the low interface state density and high breakdown field strength [2,3,7,11]. However, there are still very few studies focused on Ga₂O₃ dielectrics prepared directly on III-V NWs since the typical thermal oxidizing method is challenging to be executed on the small-diameter NWs, while the atomic-layer-deposited (ALD) high-κ HfO₂ and Al₂O₃ dielectrics often have significant interfacial defects when performed on NW materials [12]. In this case, it is necessary to explore

* Correspondence: johnnyho@cityu.edu.hk
[1]Department of Physics and Materials Science, City University of Hong Kong, 83 Tat Chee Ave., Hongkong SAR, People's Republic of China
[3]Shenzhen Research Institute, City University of Hong Kong, Shenzhen 518057, People's Republic of China
Full list of author information is available at the end of the article

other alternative dielectrics such as Ga_2O_3 achieved by other advanced techniques in order to tackle this issue for the versatile high-mobility III-V NW devices.

Among many Ga_2O_3 phases, the monoclinic β-Ga_2O_3 is the most stable phase, being a promising gate dielectric alternative; nevertheless, it often requires synthesis at high temperatures to maintain its excellent crystallinity. For example, β-Ga_2O_3 NWs are usually prepared at above 1,000°C, employing Ga metal as the source in the chemical vapor deposition (CVD) [13], and sometimes even high-energy arc plasma is utilized when using GaN as the starting material [14]. As most III-V NWs are synthesized at a moderate temperature in the range 400°C to 600°C via vapor-liquid-solid (VLS) and/or vapor-solid-solid (VSS) mechanisms [15-18], a compatible low-temperature β-Ga_2O_3 growth technique is therefore essential to grow dielectrics laterally on III-V NWs while not degrading the III-V NW materials with high vapor pressures.

Recently, we have adopted various III-V material powders as precursor sources for the NW growth by CVD, such as obtaining GaAs, InP, GaSb, etc. at a temperature of 500°C to 600°C [19-21]. Here, in this report, we perform detailed studies on the synthesis behaviors and fundamental physical properties of β-Ga_2O_3 NWs at this moderate growth temperature in a similar CVD growth system. It is revealed that highly crystalline and insulating β-Ga_2O_3 NWs are successfully grown on the amorphous SiO_2 substrate, which provides a preliminary understanding of the β-Ga_2O_3 NWs attained by the solid-source CVD method, and further enables us to manipulate the process parameters to achieve high-quality gate dielectrics laterally grown on III-V semiconductor NWs for the coaxially gated NW device structures [22].

Methods

Synthesis of Ga_2O_3 NWs

The Ga_2O_3 NWs were synthesized in a dual-zone horizontal tube furnace, where the upstream zone was used for evaporating the solid source and the downstream zone for the NW growth, as reported previously [15]. At first, 50-nm Au colloids (standard deviation of approximately 5 nm, NanoSeedz, Hong Kong) were drop-casted on SiO_2/Si substrates (50-nm thermally grown oxide) to serve as the catalyst, which were then placed in the middle of the downstream zone with a tilt angle of approximately 20°. The solid source, GaAs powders (approximately 1.0 g), was contained in a boron nitride crucible, which was then positioned in the upstream zone with a distance of approximately 10 cm away from the substrate with catalysts. During the NW growth, the substrate was initially heated to the preset growth temperature (580°C to 620°C) and the source was then heated to the required source temperature (900°C). Mixture of argon (Ar, 99.9995% purity, 100 sccm) and oxygen (O_2, 99.9995% purity) in different flow ratios (100:1 to 100:100) was used as the carrier gas to transport the thermally vaporized precursors to the downstream. After the growth of 1 h, the source and substrate heater were stopped together and cooled down to room temperature under the Ar and O_2 flow.
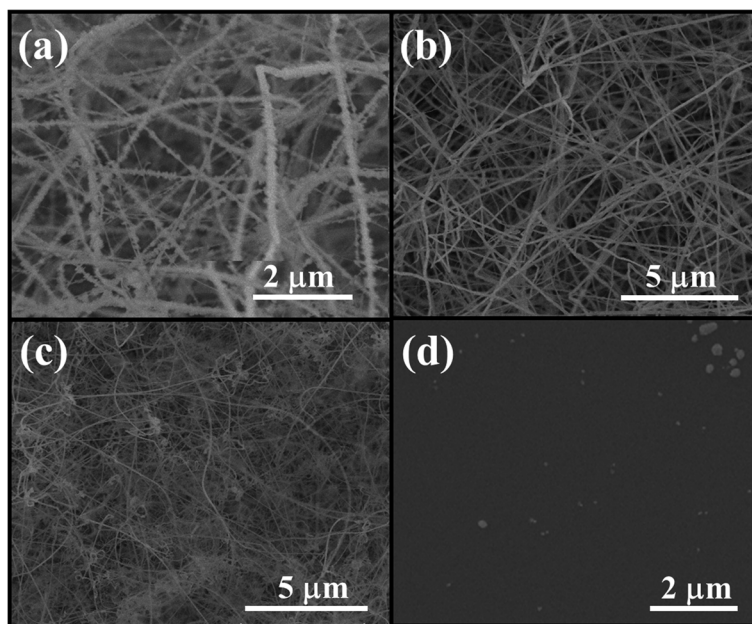

Figure 1 SEM images of the Ga_2O_3 NWs grown at different Ar:O_2 flow ratios. Source temperature at 900°C, substrate temperature at 610°C, Ar flow of 100 sccm. **(a)** 100:1. **(b)** 100:2. **(c)** 100:10. **(d)** 100:100.

Characterization of Ga_2O_3 NWs

Surface morphologies of the grown Ga_2O_3 NWs were examined with a scanning electron microscope (SEM; FEI/Philips XL30, Hillsboro, OR, USA) and transmission electron microscope (TEM; Philips CM-20, Amsterdam, The Netherlands). Crystal structures were determined by collecting X-ray diffraction (XRD) patterns on a Philips powder diffractometer using Cu Kα radiation ($\lambda = 1.5406$ Å) and by selected area electron diffraction (SAED; Philips CM-20). Elemental analysis was performed using an energy-dispersive X-ray (EDS) detector attached to JEOL CM-20 (Akishima-shi, Japan) to measure the chemical composition of the grown NWs. For the TEM and EDS analyses, the Ga_2O_3 NWs were first suspended in an ethanol solution by ultrasonication and drop-casted onto a copper grid for the corresponding characterization. The reflectance spectrum was measured with a LAMBDA 750 spectrophotometer (PerkinElmer, Waltham, MA, USA) at room temperature.

The Ga_2O_3 NW arrays were fabricated by contact printing on SiO_2/Si substrates (50-nm thermally grown oxide) as reported previously [23]. Typically, a pre-patterned SiO_2/Si substrate coated with a photoresist was used as the receiver, while the donor NW chip was flipped onto the receiver and slid at a rate of 10 mm/min with a pressure of 50 g/cm^2. After photoresist removal, the Ga_2O_3 NW arrays were left on the patterned region. Then, photolithography was utilized to define the electrode regions, and a 100-nm-thick Ni film was thermally deposited as the contact electrode followed by a lift-off process. The electrical performance of the fabricated NW arrays was characterized with a standard electrical probe station and Agilent 4155C semiconductor analyzer (Santa Clara, CA, USA).

Results and discussion

As reported previously, we synthesized GaAs NWs by the solid-source CVD method using GaAs powders as the source material heated at 900°C and 100-sccm H_2 as the carrier gas, catalyzed by Au nanoparticles at 580°C to 620°C [15,24]. In an attempt to prepare Ga_2O_3 in a compatible circumstance, we employ the same conditions here except the H_2 carrier gas, which is substituted by a mixture of Ar and O_2 in order to introduce oxygen into the growth environment. The flow rate of Ar is fixed at 100 sccm, and the ratio of Ar and O_2 is precisely tailored as 100:1, 100:2, 100:10, and 100:100 by using mass flow controllers (the pressure is approximately 0.8, approximately 0.8, approximately 0.9, and approximately 1.4 Torr, respectively). The corresponding obtained NW products appeared whitish on the substrate, in contrast with the yellowish-green GaAs NWs. The NWs are then observed by SEM as shown in Figure 1a,b,c,d. It is clear that the NWs grown at the Ar:O_2 flow ratio of 100:2 are relatively long and smooth on the surface (Figure 1b), while the lower O_2 flow induces

a significant coating problem (Figure 1a) and the higher O_2 flow suppresses the NW growth (Figure 1c,d). The high O_2 flow might deactivate the Au catalyst leading to no NW growth, while the low O_2 flow might not make the Ga_2O_3 NW nucleation sufficient over the GaAs NW growth but only overcoat on the GaAs NW surface resulting in the overcoating problem. Notably, in our former study of GaAs NWs, the GaAs powder source has depleted less than 0.1 g of weight after the growth, whereas the source has now depleted more than 0.5 g of weight in this Ga_2O_3 NW growth by introducing a small amount of oxygen. This would be attributed to the fact that even though Ga has a decently high vapor pressure, there is still a small amount of Ga being evaporated and transported in the H_2 atmosphere in the GaAs NW growth. On the other hand, when O_2 is introduced in the Ga_2O_3 NW growth, Ga is easily oxidized to Ga_2O [25], which has a far higher vapor pressure than that of metallic Ga, and thus can be massively evaporated and
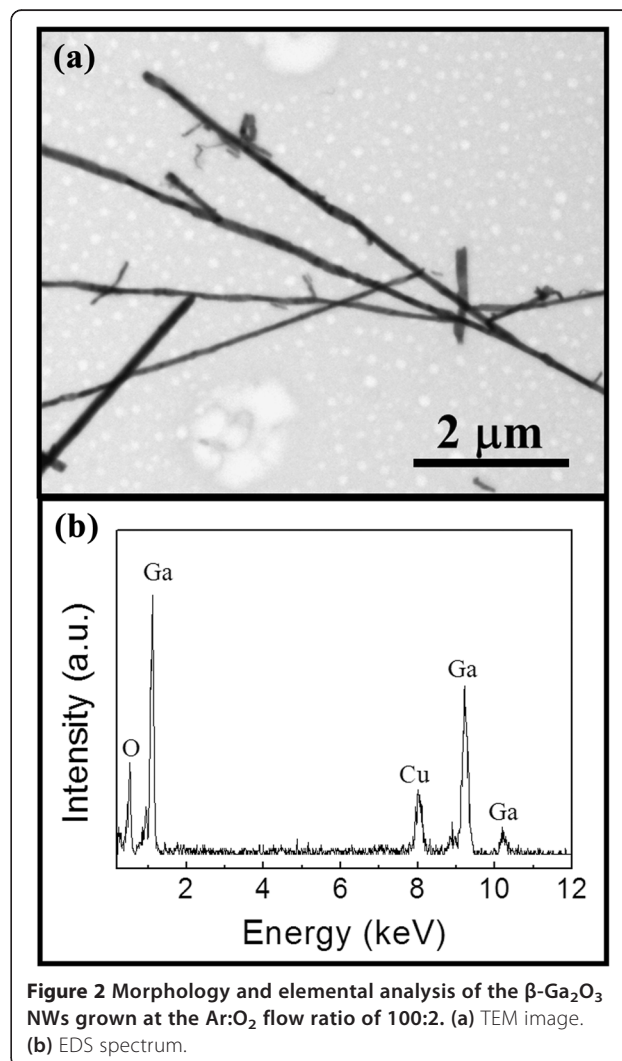

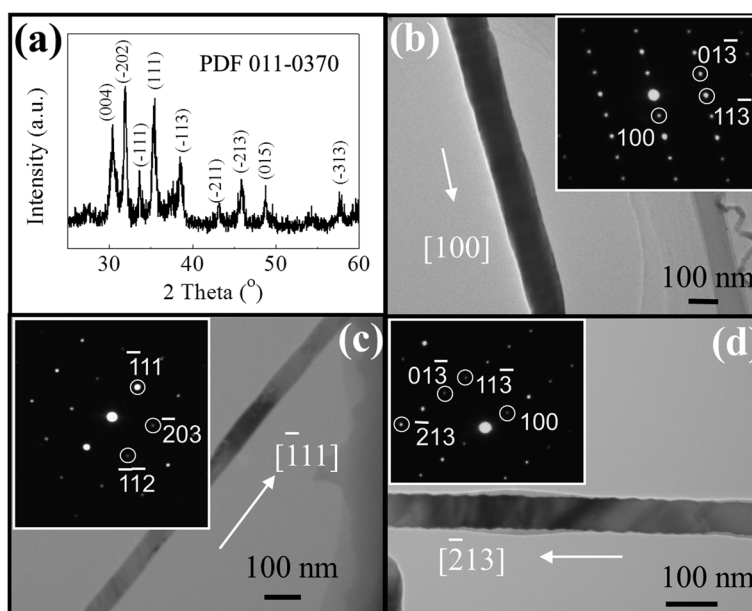**Figure 2 Morphology and elemental analysis of the β-Ga_2O_3 NWs grown at the Ar:O_2 flow ratio of 100:2. (a)** TEM image. **(b)** EDS spectrum.

Figure 3 Structural and orientation analysis of the β-Ga$_2$O$_3$ NWs grown at the Ar:O$_2$ flow ratio of 100:2. (a) XRD pattern. **(b, c, d)** TEM images and the corresponding SAED patterns (insets).

transported by the carrier gas to the substrate; as a result, a proper control in the amount of O$_2$ feed is critical for the effective NW growth here.

The NWs grown at the Ar:O$_2$ flow ratio of 100:2 are then observed by TEM as depicted in Figure 2a, which further confirms the straight NWs with smooth surfaces. Furthermore, the elemental composition is analyzed by EDS, and the typical spectrum is illustrated in Figure 2b, which clearly demonstrates that the NWs are mainly composed of Ga and O with an atomic ratio of approximately 2:3. These results evidently show that the obtained NWs here are Ga$_2$O$_3$ instead of the GaAs NWs grown in the H$_2$ atmosphere. It should also be noted that although As-doped In$_2$O$_3$ NWs were prepared in a similar system when utilizing InAs powders as the source material and As is detected in the EDS spectrum [26], no As-related signal is obtained within the detection limit of EDS performed in this study. This difference may be due to the alteration in the synthesis condition that H$_2$ is intentionally introduced into the Ar/O$_2$ carrier gas to suppress the oxide growth in [25], which can be ruled out in this Ga$_2$O$_3$ NW growth. It is plausible that since oxygen has a far higher electron negativity (approximately 3.44) than arsenic (approximately 2.18) and that Ga$_2$O$_3$ has a far lower Gibbs free energy (approximately −998.3 kJ/mol) than GaAs (−67.8 kJ/mol) [27], in this case, Ga$_2$O$_3$ is more preferentially grown from the thermal dynamics point of view. In other words, when H$_2$ in introduced, Ga$_2$O$_3$ growth would be deterred and get substituted by the GaAs growth [25].

In order to investigate the crystal structure of the obtained Ga$_2$O$_3$ NWs, the XRD pattern is attained for NWs readily grown on the SiO$_2$/Si substrate as presented in Figure 3a. It is obvious that the NWs are grown in the monoclinic structure (β-phase) in accordance with the standard card PDF 011-0370. Then, the crystal structure and growth orientation of individual NWs are further studied by using SAED as shown in Figure 3b,c,d. All these indicate that the representative NWs all existed in the monoclinic crystal structure, which is in good agreement with the XRD results. Even though the orientations are
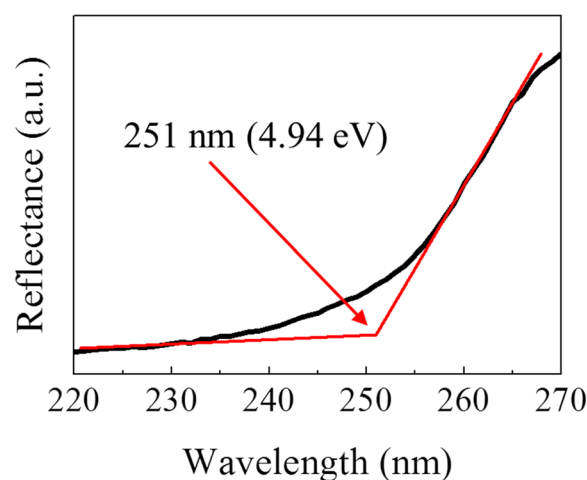

Figure 4 Reflectance spectrum of the β-Ga$_2$O$_3$ NWs grown at the Ar:O$_2$ flow ratio of 100:2.

observed to vary from NW to NW, typically low-index directions such as [100], [$\bar{1}$11], and [$\bar{2}$13] are perceived, which might have resulted from the similar surface energies of these crystal planes, especially for materials in the nanometer size with the examples reported in Si NWs [28], GaAs NWs [15], ZnSe NWs [29], etc.

The bandgap of β-Ga$_2$O$_3$ NWs can also be determined by the reflectance spectrum as depicted in Figure 4. It clearly shows that the absorption edge lies at approximately 251 nm (4.94 eV). This bandgap value is in good agreement with that of β-Ga$_2$O$_3$ NWs reported in the literature (approximately 254 nm) [30] while a bit higher than that of bulk materials (approximately 270 nm) [31]. A relatively larger bandgap of nanomaterials is often observed than their bulk counterparts, which is usually attributed to the quantum confinement effect of nanomaterials, inducing a blueshift of the bandgap [32].

To shed light on exploring the electronic properties of achieved β-Ga$_2$O$_3$ NWs, the resistance of NWs is first assessed by defining electrodes by standard photolithography. It should be noted that when defining Ni electrodes on a single β-Ga$_2$O$_3$ NW, no significant current can be obtained as compared with the resolution (approximately 1 pA) of our semiconductor analyzer and probe station. In order to enlarge the current signal to a measurable level, the β-Ga$_2$O$_3$ NWs are then aligned into parallel arrays by the contact printing technique as reported previously [8,23]. Ni electrodes (with the work function of approximately 5.1 eV) are then defined on both ends of the NW arrays, given in the SEM image in Figure 5a. The NW density is approximately 1 NW/μm, accounting for approximately 200 NWs in the 200 μm (width) × 3.7 μm (length) channel area. In this way, the current-voltage (*I-V*) curve of the representative β-Ga$_2$O$_3$ NW array is measured and shown in Figure 5b, where the resistance is estimated to be approximately 2×10^{12} Ω as the current is approximately 5 pA under 10-V bias. As a result, the resistance is approximately 4×10^{14} Ω per individual NW (approximately $2 \times 10^{12} \times 200$ Ω, as 200 NWs are connected in parallel). Then, the resistivity can be estimated as $2 \times 10^{12} \times 200$ Ω × 3.7 μm/3.14/50^2 nm$^2 = 8.5 \times 10^7$ Ω cm, considering the NW diameter of approximately 100 nm. Notably, other metal electrodes with different work functions such as Al (approximately 4.2 eV) and Au (approximately 5.3 eV) are also prepared, in which the results attained are all similar as shown in Figure 5b, suggesting the highly insulating property of the NWs here. This resistivity is relatively larger than those of doped and undoped β-Ga$_2$O$_3$ NWs reported in the literature [4,6,13], which can be attributed to the moderate growth temperature employed in this work such that less impurity would be incorporated, showing its prospective in dielectric materials for advanced III-V nanowire-based nanoelectronics.
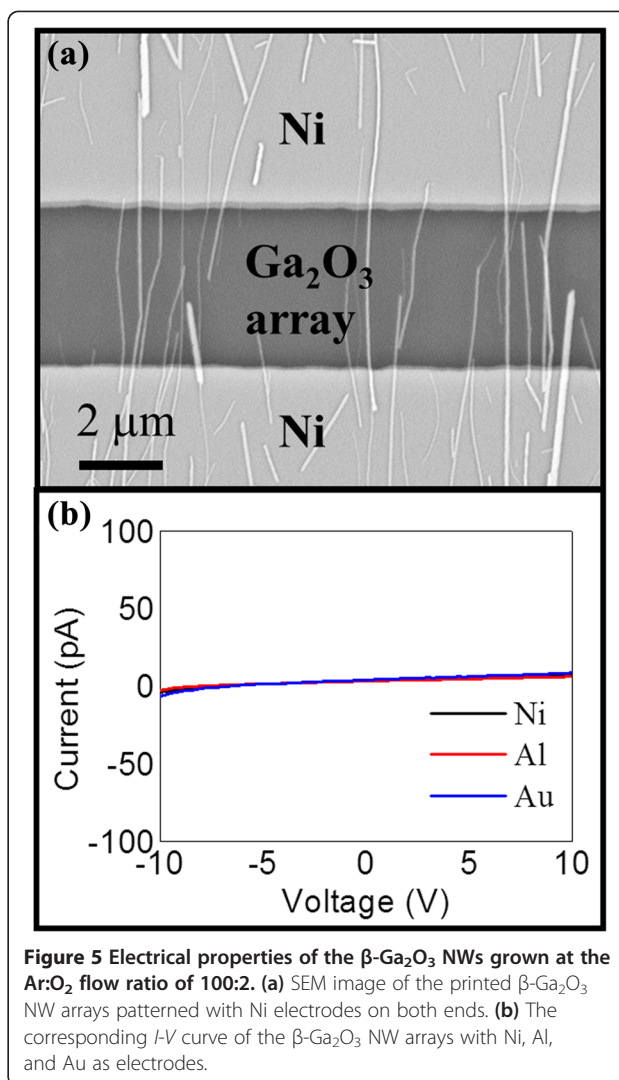

Figure 5 Electrical properties of the β-Ga$_2$O$_3$ NWs grown at the Ar:O$_2$ flow ratio of 100:2. (a) SEM image of the printed β-Ga$_2$O$_3$ NW arrays patterned with Ni electrodes on both ends. **(b)** The corresponding *I-V* curve of the β-Ga$_2$O$_3$ NW arrays with Ni, Al, and Au as electrodes.

Conclusions

Highly crystalline β-Ga$_2$O$_3$ NWs are synthesized by a solid-source chemical vapor deposition method employing GaAs powders as the source material and mixture of Ar and O$_2$ as the carrier gas. The NWs grown at the Ar:O$_2$ flow ratio of 100:2 are long (>10 μm) with a uniform diameter of approximately 100 nm and smooth surfaces. X-ray diffraction and selected area electron diffraction results confirm the monoclinic structure of the obtained NWs with varied growth orientations along the low-index planes. Furthermore, the reflectance spectrum demonstrates the bandgap of β-Ga$_2$O$_3$ NWs being 4.94 eV, while the electrical measurement deduces the corresponding resistivity of 8.5×10^7 Ω cm. All these results indicate the successful synthesis of a large-bandgap Ga$_2$O$_3$ material in III-V-compatible growth conditions, illustrating the promising potential for dielectric materials used for III-V nanowire-based metal-oxide-semiconductor technology.

Competing interests

The authors declare that they have no competing interests.

Authors' contributions

NH synthesized the Ga_2O_3 NWs and drafted the manuscript. FW made the SEM and TEM observations, ZY carried out the XRD measurement, and SY carried out the reflectance spectrum. GD fabricated the NW array devices, and HL made the I-V measurement. MF made the SAED identification, and TH carried out the EDS spectrum. JCH provided the idea and completed the manuscript. All authors read and approved the final manuscript.

Acknowledgements

Author details

[1]Department of Physics and Materials Science, City University of Hong Kong, 83 Tat Chee Ave., Hongkong SAR, People's Republic of China. [2]Cultivation Base for State Key Laboratory, Qingdao University, No. 308 Ningxia Road, Qingdao 266071, People's Republic of China. [3]Shenzhen Research Institute, City University of Hong Kong, Shenzhen 518057, People's Republic of China.

References

1. Lin TD, Chiu HC, Chang P, Tung LT, Chen CP, Hong M, Kwo J, Tsai W, Wang YC: High-performance self-aligned inversion-channel $In_{0.53}Ga_{0.47}As$ metal-oxide-semiconductor field-effect-transistor with Al_2O_3/Ga_2O_3 (Gd_2O_3) as gate dielectrics. Appl Phys Lett 2008, 93:033516.
2. Paterson GW, Wilson JA, Moran D, Hill R, Long AR, Thayne I, Passlack M, Droopad R: Gallium oxide (Ga_2O_3) on gallium arsenide - a low defect, high-K system for future devices. Mat Sci Eng B-Solid 2006, 135:277–281.
3. Ren F, Kuo JM, Hong M, Hobson WS, Lothian JR, Lin J, Tsai HS, Mannaerts JP, Kwo J, Chu SNG, Chen YK, Cho AK: $Ga_2O_3(Gd_2O_3)$/InGaAs enhancement-mode n-channel MOSFETs. IEEE Electr Device L 1998, 19:309–311.
4. Oshima T, Okuno T, Arai N, Suzuki N, Ohira S, Fujita S: Vertical solar-blind deep-ultraviolet Schottky photodetectors based on β-Ga_2O_3 substrates. Appl Phys Express 2008, 1:011202.
5. Weng WY, Hsueh TJ, Chang SJ, Huang GJ, Hung SC: Growth of Ga_2O_3 nanowires and the fabrication of solar-blind photodetector. IEEE T Nanotechnol 2011, 10:1047–1052.
6. Feng P, Zhang JY, Li QH, Wang TH: Individual β-Ga_2O_3 nanowires as solar-blind photodetectors. Appl Phys Lett 2006, 88:153107.
7. Passlack M, Droopad R, Rajagopalan K, Abrokwah J, Zurcher P, Fejes P: High mobility III-V MOSFET technology. In CSIC 2006, IEEE Compound Semiconductor Integrated Circuit Symposium: November 2006. Edited by San Antonio: IEEE; 2006:39–42.
8. Han N, Wang FY, Hou JJ, Yip SP, Lin H, Xiu F, Fang M, Yang ZX, Shi XL, Dong GF, Hung TF, Ho JC: Tunable electronic transport properties of metal-cluster-decorated III-V nanowire transistors. Adv Mater 2013, 25:4445–4451.
9. Chueh Y-L, Ford AC, Ho JC, Jacobson ZA, Fan Z, Chen C-Y, Chou L-J, Javey A: Formation and characterization of Ni_xInAs/InAs nanowire heterostructures by solid source reaction. Nano Letters 2008, 8:4528–4533.
10. Robertson J: High dielectric constant gate oxides for metal oxide Si transistors. Rep Prog Phys 2006, 69:327–396.
11. Kim H, Park SJ, Hwang HS: Thermally oxidized GaN film for use as gate insulators. J Vac Sci Technol B 2001, 19:579–581.
12. del Alamo JA: Nanometre-scale electronics with III-V compound semiconductors. Nature 2011, 479:317–323.
13. Chang PC, Fan ZY, Tseng WY, Rajagopal A, Lu JG: β-Ga_2O_3 nanowires: synthesis, characterization, and p-channel field-effect transistor. Appl Phys Lett 2005, 87:222102.
14. Choi YC, Kim WS, Park YS, Lee SM, Bae DJ, Lee YH, Park GS, Choi WB, Lee NS, Kim JM: Catalytic growth of β-Ga_2O_3 nanowires by arc discharge. Adv Mater 2000, 12:746–750.
15. Han N, Wang F, Hou JJ, Yip S, Lin H, Fang M, Xiu F, Shi X, Hung T, Ho JC: Manipulated growth of GaAs nanowires: controllable crystal quality and growth orientations via a supersaturation-controlled engineering process. Cryst Growth Des 2012, 12:6243–6249.
16. Persson AI, Larsson MW, Stenstrom S, Ohlsson BJ, Samuelson L, Wallenberg LR: Solid-phase diffusion mechanism for GaAs nanowire growth. Nat Mater 2004, 3:677–681.
17. Hou JJ, Han N, Wang F, Xiu F, Yip S, Hui AT, Hung T, Ho JC: Synthesis and characterizations of ternary InGaAs nanowires by a two-step growth method for high-performance electronic devices. ACS Nano 2012, 6:3624–3630.
18. Yang ZX, Han N, Wang FY, Cheung HY, Shi XL, Yip S, Hung T, Lee MH, Wong CY, Ho JC: Carbon doping of InSb nanowires for high-performance p-channel field-effect-transistors. Nanoscale 2013, 5:9671–9676.
19. Han N, Hou JJ, Wang FY, Yip S, Yen YT, Yang ZX, Dong GF, Hung T, Chueh YL, Ho JC: GaAs nanowires: from manipulation of defect formation to controllable electronic transport properties. ACS Nano 2013, 7:9138–9146.
20. Hui AT, Wang F, Han N, Yip SP, Xiu F, Hou JJ, Yen YT, Hung TF, Chueh YL, Ho JC: High-performance indium phosphide nanowires synthesized on amorphous substrates: from formation mechanism to optical and electrical transport measurements. J Mater Chem 2012, 22:10704–10708.
21. Yang ZX, Wang FY, Han N, Lin H, Cheung HY, Fang M, Yip S, Hung TF, Wong CY, Ho JC: Crystalline GaSb nanowires synthesized on amorphous substrates: from the formation mechanism to p-channel transistor applications. ACS Appl Mat Interfaces 2013, 5:10946–10952.
22. Kim BK, Kim JJ, Lee JO, Kong KJ, Seo HJ, Lee CJ: Top-gated field-effect transistor and rectifying diode operation of core-shell structured GaP nanowire devices. Phys Rev B 2005, 71:153313.
23. Fan ZY, Ho JC, Takahashi T, Yerushalmi R, Takei K, Ford AC, Chueh YL, Javey A: Toward the development of printable nanowire electronics and sensors. Adv Mater 2009, 21:3730–3743.
24. Han N, Wang F, Hou JJ, Xiu F, Yip S, Hui AT, Hung T, Ho JC: Controllable p-n switching behaviors of GaAs nanowires via an interface effect. ACS Nano 2012, 6:4428–4433.
25. Shi WS, Zheng YF, Wang N, Lee CS, Lee ST: A general synthetic route to III-V compound semiconductor nanowires. Adv Mater 2001, 13:591–594.
26. Chen PC, Shen GZ, Chen HT, Ha YG, Wu C, Sukcharoenchoke S, Fu Y, Liu J, Facchetti A, Marks TJ, Thompson ME, Zhou CW: High-performance single-crystalline arsenic-doped indium oxide nanowires for transparent thin-film transistors and active matrix organic light-emitting diode displays. ACS Nano 2009, 3:3383–3390.
27. Speight JG: Lange's Handbook of Chemistry. New York: McGraw-Hill; 2005.
28. Schmidt V, Senz S, Gösele U: Diameter-dependent growth direction of epitaxial silicon nanowires. Nano Lett 2005, 5:931–935.
29. Cai Y, Chan SK, Soar IK, Chan YT, Su DS, Wang N: The size-dependent growth direction of ZnSe nanowires. Adv Mater 2006, 18:109–114.
30. Feng P, Xue XY, Liu YG, Wan Q, Wang TH: Achieving fast oxygen response in individual β-Ga_2O_3 nanowires by ultraviolet illumination. Appl Phys Lett 2006, 89:112114.
31. Tippins H: Optical absorption and photoconductivity in the band edge of β-Ga_2O_3. Phys Rev 1965, 140:A316.
32. Zhang GQ, Tateno K, Sanada H, Tawara T, Gotoh H, Nakano H: Synthesis of GaAs nanowires with very small diameters and their optical properties with the radial quantum-confinement effect. Appl Phys Lett 2009, 95:123104.